https://doi.org/10.5194/egusphere-2023-1394
Preprint. Discussion started: 7 July 2023

Links between seasonal suprapermafrost groundwater, the hydrothermal change of the active layer, and river runoff in alpine permafrost watersheds

Jia Qin[1,2], Yongjian Ding[1,2], Tianding Han[1,2], Faxiang Shi[1,2], Qiudong Zhao[2,3],Yaping Chang[1,3], Junhao Cui[1,2]

[1] State Key Laboratory of Cryospheric Sciences, Northwest Institute of Eco-Environment and Resources, Chinese Academy of Sciences, Lanzhou, 730000, China
[2] University of Chinese Academy of Sciences, Beijing, 100049, China
[3] Key Laboratory of Eco-hydrology Inland River Basin, Northwest Institute of Eco-Environment and Resources, Chinese Academy of Sciences, Lanzhou, 730000, China

Correspondence to: Yongjian Ding (dyj@lzb.ac.cn)

Abstract. The seasonal dynamic of suprapermafrost groundwater significantly affects runoff generation and concentration in permafrost basins and is a leading issue that must urgently be addressed in hydrological research in cold and alpine regions. In this study, the seasonal dynamic process of the suprapermafrost groundwater level (SGL), vertical gradient changes of soil temperature (ST) and moisture content in the active layer (AL), and river level changes were systematically analyzed at four permafrost watersheds in the Qinghai–Tibet Plateau using comparative analysis and the nonlinear correlation evaluation method. How freeze–thaw processes impact seasonal SGL, and the links between SGL and surface runoff, were also discussed. The SGL process in a hydrological year can be divided into four periods: (A) a rapid falling period (October–middle November), (B) a stable low-water period (late November–May), (C) a rapid rising period (approximately June), and (D) a stable high-water period (July–September), which synchronously respond to seasonal variations in soil moisture and temperature in the AL. The characteristics and causes of SGL changes varied significantly during the four different periods. The freeze-thaw process of the AL has crucial regulatory effects on SGL and surface runoff in permafrost watersheds. During Period A, with rapid AL freezing, the ST had a dominant impact on the SGL. In Period B, the AL was entirely frozen because of the stably low ST, and the SGL dropped to the lowest level with small changes. During Period C, ST in the deep soil layers of the active layer (below 50 cm depth) significantly impacted the SGL (nonlinear correlation coefficient R^2>0.74, P<0.05), whereas the SGL change in the shallow soil layer (0–50 cm depth) had a closer relationship with soil moisture content. Rainfall was the major cause for the stable high SGL during Period D. In addition, the SGLs in Periods C and D were closely linked to the retreat and flood processes of river runoff. The SWL contributed approximately 57.0–65.8 % of the river runoff changes in Period D. These findings can provide references for hydrological research in permafrost basins and guide the rational development and utilization of water resources in cold and alpine regions.

https://doi.org/10.5194/egusphere-2023-1394
Preprint. Discussion started: 7 July 2023

1 Introduction

The suprapermafrost groundwater (SG) refers to groundwater distributed above the permafrost layer, and its stable floor is the permafrost table, which is primarily recharged by rainfall, surface water, and lateral flow in the active layer (AL) (Ma et al., 2017; Tregubov et al., 2022). When the surface soil is frozen, most surface recharge sources of the SG are cut off, whereas, during the summer thawing season, the SG becomes non-confined water with a free surface (Qin et al., 2016). SG significantly impacts the regional water cycle and the supply-demand relationship of ecological water in permafrost watersheds (Huang et al., 2020; Gao et al., 2021). It plays a crucial role in the research on land surface processes and hydrology in cold regions (Wellman et al., 2013; Chang et al., 2015; Liu et al., 2021).

The SG maintains a high value during the summer half-year because of the quantity of rainfall and surface water frequently infiltrating the thawed AL (Cao et al., 2021; Tregubov et al., 2021). The suprapermafrost groundwater level (SGL) dynamic is directly affected by rainfall and the surface meltwater supply (Young et al., 2000). Because of the impermeability of the permafrost table, SG can flow out of low-lying areas after reaching a particular level or directly supply river runoff or lakes laterally (Krickov et al., 2018; O'Neill et al., 2020; Gao et al., 2021; Qin et al., 2022). In the winter half of the year, with decreasing air temperature and surface soil freezing, most SG turn into ground ice stored in the AL (Xu et al., 2021). As a type of groundwater, SG has a crucial impact on the hydrological processes and water cycles in permafrost basins through water migration and transformation (Ge et al., 2011; Chen et al., 2018). As one of the primary water sources for lake and river runoff in a permafrost basin, the SG cannot be disregarded, especially during the summer AL thawing period. In some continuous permafrost basins, such as the source area of the Shule River in the northeastern part of the Qinghai–Tibet Plateau, SG contributes to over 30 % of the total river runoff (Qin et al., 2022). The SG recharged over 60 mm of water into the thermokarst lake in the Beiluhe watershed of the Qinghai–Tibet Plateau from June 20 to October 26, 2019, when the surface runoff flow into the thermokarst lake was only approximately 170 mm (Gao et al., 2021). The effect of frozen SG in the winter half of the year can also not be disregarded because the ice stored in AL could rapidly thaw in spring and supply a substantial amount of water to the spring flood. For example, at least one-third of the Shestakovka River spring flood is formed by melted superpermaforst ice (Lebedeva, 2019), and the measured SG contributes to over 60 % of the total discharge in the Ugol'naya-Dionisiya River at the beginning of the warm season (Tregubov et al., 2021). In addition, SG is a major source of baseflow in cold river basins. Simulation analysis shows that the contribution of SG to base flow is over 90 % in the continuous permafrost region of the Yukon River Basin around the Arctic (Walvoord et al., 2012).

Permafrost thaw is closely linked to soil moisture and temperature (Schuur and Abbott, 2011). The dynamics of SG are closely related to the seasonal hydrothermal changes and freeze–thaw process of AL. With the freezing–thawing–refreezing of the AL, the SGL correspondingly has a distinct response (Ye and Juan, 2019), which is a significant hydrological characteristic that differs from that in non-frozen soil regions (Cao et al., 2018). Existing studies regarding seasonal SG focus on the characteristics of SG change in different freeze–thaw stages of AL in basins of the high latitudes of the Northern Hemisphere and Qinghai–Tibet Plateau (Chang et al., 2015; Throckmorton et al., 2016; O'Connor et al., 2019; Cao

https://doi.org/10.5194/egusphere-2023-1394
Preprint. Discussion started: 7 July 2023

et al., 2021) and the impact factors of SG variation, including the climate (such as rainfall and air temperature (Dugan et al., 2009; Zhang et al., 2021), geological conditions (Woo and Xia, 1995; Sjöberg et al., 2013), soil properties (Raudina et al., 2018), and vegetation types (Koch et al., 2022), as well as the slope and aspect of the permafrost watershed (Cao et al., 2003; Tregubov et al., 2021).

Existing studies have enhanced the understanding of SG, and its effect has improved the development of permafrost hydrology. However, there is a shortfall in systematically revealing the linkage between the seasonal hydrothermal change of AL, SG, and surface runoff. This unclear linkage, which has been regarded as a "black box" in hydrological analyses and simulations, is a bottleneck problem in permafrost hydrological studies. Identifying seasonal variations in SG and its hydrological linkages based on systematic experimental observations is essential in cold regions, especially in the context of climate warming.

To further understand the dynamic rules and driving factors of SG, this study selected continuous permafrost watersheds in different locations of the Qinghai–Tibet Plateau to explore two scientific problems: (1) the seasonal dynamic pattern and spatial differentiation law of SG and (2) the influence of the AL freeze–thaw process on the dynamic changes in SG and river runoff in permafrost watersheds. Based on field observations, this study attempted to reveal the seasonal variation patterns of SG, aiming to provide scientific and theoretical support for regional water cycle research in permafrost regions.

2 Study area and materials

2.1 Selected research stations

Four permafrost stations were selected in this study (HLG, SL, MD, and FHS) at different locations on the Qinghai–Tibet Plateau (Fig. 1) to conduct a comparative analysis of the meteorological and hydrothermal changes in AL and river runoff. The HLG experimental station and SL station are located in the headwater regions of the Heihe and Shule Rivers in the Qilian Mountains of the northeastern Qinghai–Tibet Plateau, respectively, and the MD and FHS stations are in the headwater regions of the Yellow and Yangtze Rivers in the hinterland of the Qinghai–Tibet Plateau. The mean annual precipitation at these four stations ranges from 100 to 400 mm. Stations HLG and SL in the Qilian Mountains have higher annual precipitation than stations FHS and MD. The annual precipitation at the HLG station is the highest (403.4 mm), whereas that at the MD station is 133.7 mm. The mean annual temperature in the four stations ranges from –5.2 ℃ (FHS) to 2 ℃ (MD), and their ground temperature ranges from –1.7 ℃ (FHS) to 0.3 ℃ (HLG). The maximum AL thawing depth at the research sites changes from 1 m at the SL observation station to 2.5 m at the FHS station in summer. The primary vegetation types on the underlying surfaces of the stations are alpine meadows, alpine grasslands, and swamp meadows.

https://doi.org/10.5194/egusphere-2023-1394
Preprint. Discussion started: 7 July 2023

2.2 Experimental data

This study was primarily based on soil temperature (ST) and soil volumetric moisture content (SVMC) measured at different depths of AL, as well as the SGL data at the four permafrost stations (Fig. 4). The analysis of ST, SVMC, and SGL was conducted in a hydrological year (from October 1 to September 30), and the time scale was daily. These data were obtained from the field observation stations of the Chinese Academy of Sciences and from existing literature (Chang et al., 2015; Cao et al., 2018; Qin et al., 2022). The daily data of the river level (RL) during the wet season (in summer) and water recession period (in autumn) in SL and FHS watersheds was also measured and compared with SGL to analyze the "SGL-RL" dynamic relationship. Daily rainfall data for the same hydrological year were obtained from automatic rain and snow gauges (T-200B) (30 min) at the permafrost stations and nearby national weather stations (http://data.cma.cn/).

2.3 Observation of soil hydrothermal change and SGL

ST and SVMC at different AL depths were the two major soil hydrothermal parameters used in this study. In SL and HLG stations, they were continuously measured using HydraProbe Lite sensors with an accuracy of 0.3 °C and ±1.0 %. The ST in the MD and FHS stations were measured by S-TMB-M006 sensors with an accuracy of 0.2 °C, and the SVMC was measured by S-SMC-M005 sensors with an accuracy of ±3.0 %. All sensors are suitable for use at –40 °C -50 °C. All probes used for measuring the ST and SVMC were buried in the soil from the ground surface (10 cm depth) to the permafrost table. Probes were installed in the soil at depths of 10, 20, 40, 60, 80, 120, and 160 cm. All instruments were attached to a CR1000 data logger for data acquisition at each station, and recorded data were collected once every 30 min.

The SGLs at the four stations were measured using a HOBO pressure water level logger (U 20-001-04) produced in the United States. The logger is a built-in pressure water level sensor with a fully enclosed titanium alloy shell. It is suitable for the automatic observation of groundwater in alpine environments. The measurement accuracy was high, with a resolution of 0.014 kPa (0.14 cm water depth). A water level logger was set in the AL groundwater wells at the four stations, and data were automatically collected every 30 min. The HOBOware Pro software was used to operate the logger. Using a reference water level, HOBOware Pro automatically converts pressure readings into water level readings, and the SGL data for a specific measurement period can be obtained. In addition, some data from manually measuring the groundwater level with a ruler were used to compare and correct the HOBO-observed SGL data in different wet and dry periods. Daily SGL was calculated by averaging all corrected water level data every 30 min for each day.

2.4 Correlation analysis between the SGL and soil hydrothermal parameters in the AL

A contour map was created using SigmaPlot (SigmaPlot 14.0, 2020) software to analyze the ST and SVMC changes at different depths of the AL. To analyze the impact of soil hydrothermal parameters on SGL, the Levenberg–Marquardt method and Universal Global Optimization algorithm were used to perform nonlinear fitting between ST and SGL as well as

https://doi.org/10.5194/egusphere-2023-1394
Preprint. Discussion started: 7 July 2023

between SVMC and SGL. In addition, SPSS (SPSS 18.0, 2016) was used to perform nonlinear correlation analysis. The fitting and correlations were evaluated using the coefficient of determination (R^2) and residual standard error.

3 Seasonal characteristics of SG

Figure 2 shows the seasonal SGL at different stations on the Qinghai–Tibet Plateau. There are four typical periods of variation throughout the hydrological year. According to the tip points, which refer to the start or end times of different periods, the four periods of the SGL can be divided as follows: (A) rapid falling period, (B) stable low-water period, (C) rapid rising period, and (D) stable high-water period. Periods A–D began in mid-autumn (October–early November), early winter (late November–early December), early summer (June), and mid-summer (July). The specific start and end time of each period, as well as the duration of each period, showed minimal difference among the four stations (Fig. 2).

The SGL shown in Fig. 2 has a synchronous response to seasonal variations in ST and SVMC in the AL (Fig. 3). ST rapidly decreases to zero (rapid freezing), stable low temperature below 0 ℃ (frozen stability), rapid rising above 0 ℃ (rapid thawing), and fluctuation above 0 ℃ (thawing stability) in Periods A, B, C, and D, respectively. The SVMC also has four corresponding stages: rapid reduction, stable low value, rapid rise, and fluctuation with the complete melting of the AL.

According to the vertical variations in seasonal SVMC and SGL at the experimental sites (Fig. 3), summer SGL fluctuates at depths where SVMC has a high value. For example, the summer SGL at the SL site primarily fluctuated at 40–60 cm depths, where the SVMC also has a high value, and the soil remains saturated or nearly saturated for an extended duration. Similar to the SL station, the summer SGL at the MD station fluctuates in 10–80 cm depths, where the SVMC also maintained a higher value (Fig. 2). To some extent, SVMC could be a dynamic indicator of SGL. Exploring the soil characteristics and SVMC in the AL can indirectly clarify the SGL dynamics in a specific area.

The SGL in Period D responded rapidly to rainfall and dropped to a low value when no rainfall occurred (Fig. 2). It is inferred that precipitation is a major water source that recharges SG during the thawing stability period of AL. Currently, AL reaches its maximum depth in a year, and SGL is stable at a high groundwater level. For example, the SGL in Period D was stable above 80 cm depth at the SL station, rising rapidly when rainfall occurred and reducing slowly to a stable level after rainfall (Fig. 2). The delayed SGL falling after a rain event shows that AL has a distinct role in water conservation and can significantly regulate soil water transport and runoff processes in a permafrost watershed. This water-conservation effect is crucial for alpine ecosystems.

4 Impact of ST and SVMC on SG in the study area

To further detect the impacts of the seasonal freeze–thaw process of AL on SGL, detailed relationships between SGL and ST, as well as SVMC at different AL depths, were analyzed. Figs. 4 and 5 show the correlations between SVMC and SGL, as well as between ST and SGL, in different soil layers at the SL station.

https://doi.org/10.5194/egusphere-2023-1394
Preprint. Discussion started: 7 July 2023

During Periods A (also the rapid freezing period of AL) and C (also the rapid thawing period of AL), the relationship between SG and ST in AL could be described using the Sigmoid–Boltzmann formula (Wang et al., 2012). For example, the nonlinear relationships between the measured ST and SG fit well (R^2>0.8, P<0.01) in both periods (except for the–0–50 cm shallow soils in Period C) at the SL station (Fig. 4). The Sigmoid–Boltzmann formula is expressed as follows:

$$H = H_0 + \frac{a}{1 + e^{-\left(\frac{T-T_0}{b}\right)}}$$

H represents the SGL, and T and T_0 represent the ST of the target depths and the initial ST during the calculation period at that depth, respectively (unit: ℃); H_0 represents the initial SGL, and a and b are undetermined parameters that are related to soil characteristics at different depths.

During Period C, there was no significant relationship between ST and SGL at depths of 10, 30, and 50 cm (P>0.05). ST at 70, 90, 120, and 160 cm depths had a significant effect on SGL (P<0.01). However, the overall correlation between ST and SGL improved with increasing depth, and the impact of ST on SGL became more significant (Fig. 4a). The shallow soils (0–50 cm) in AL rapidly thawed in the initial stage of Period C, with the SGL rising rapidly, which was caused by multi-source water recharge, including the lateral flow from thawed soils, rainfall and snowmelt infiltration, and adjacent spring river floods. In the subsequent stage of Period C, soil water replenishment was relatively stable, and SGL dynamics were significantly affected by the thawing depths of AL, according to the good consistency between SGL and the thawing process (Figs. 2 and 3). The SG in the deeper soil layers was more dominated by ST compared with that in the shallow soils. In addition, the variation range of ST in the different soil layers differed during Period C. As shown in Fig. 4a, the ST range in shallow soil was substantially wider than that in deep soil. During the SGL variation period, the variation range of ST at a depth of 10 cm was 3–12 ℃, while the response of SGL to ST in deep soil was more intense. For example, the fluctuation of SGL from low to high water level was completed within the range of approximately –0.5–0.5 ℃ at 160 cm (Fig. 4a). This indicates that the ST impacts SGL dynamics only after soil thawing (>–0.5 ℃).

Figure 4c shows the dynamic relationship between ST and SGL at the SL station during Period A (the rapid freezing period of AL). The results show a significant nonlinear correlation between SGL and ST at different depths ranging from 0 to 160 cm, with a determinable coefficient (R^2) ranging from 0.81 to 0.98 (P<0.05). However, significant differences were observed in the response of the SGL to the ST at different depths. For example, the range of ST at a depth of 10 cm at the SL station was approximately –10–5 ℃ corresponding to rapid changes in SGL, while it narrowed to approximately –4–4 ℃ at a depth of 50 cm,–1–4 ℃ at a depth of 90 cm, and approximately –0.2–3 ℃ at a depth of 160 cm (Figure 4c). This is consistent with the gradual decrease in ST with increasing depth, which indicates that SG is more sensitive to ST changes in the deeper AL than in the shallow layer in Period A. According to the fitting analysis shown in Figure 4c, the correlation between ST and SGL gradually increases with increasing depth. In the early stage of Period A, as the ST decreased, the soil froze gradually, and the liquid water in the soil transformed into solid ice, resulting in a decrease in the SGL. The correlation coefficient between ST and SGL was the lowest in shallow soil, especially in the soil layer of 0–10 cm depth. This indicates

https://doi.org/10.5194/egusphere-2023-1394
Preprint. Discussion started: 7 July 2023

that the impact of shallow soil freezing on the SGL was weak during the freezing process in Period A. This has a limited impact on the SGL, which can obtain a particular amount of surface water through fissure infiltration and lateral flow.

The correlations between the SGL and SVMC during Period C were also fitted to the sigmoid formula (RMSE < 10). Except for the soil layers at 70–120 cm depths, where the correlation between the SGL and SVMC was poor ($R^2 < 0.6$, $P > 0.05$), the different soil layers of AL showed a good nonlinear correlation between the SGL and SVMC ($P<0.01$) (Figure 4b). The SGL changes in soil layers at 0–50 cm depths were more correlated with the SVMC, while SGL changes in a deeper AL (70–120 cm depths) were more significantly affected by ST, with better correlation (Figure 4a, 4b). The correlation between SVMC and SGL was also very good ($R^2 = 0.93$) at the bottom of the AL (160 cm depth). The correlation patterns further confirmed that AL began to melt downwards from the surface soil during the warm season. During the rapid thawing period of AL (Period C), the shallow soil first melts and can rapidly receive water supply from rainfall and surface meltwater, which further results in the rapid response of the SGL. The SGL in a shallow soil layer has a high degree of response to SVMC change, while the thawing of deep soil in AL is primarily controlled by ST. A higher ST leads to deep soil thaws, and the water flow channels between the surface AL and deep soil can then be fully connected, resulting in SGL changing accordingly. When the deep soil insufficiently thawed, the water-resisting effect of frozen soil exists, and it is difficult to form lateral flow and saturated soil flow to recharge the SG. The water movement of the thawed soil layer (including saturated soil flow) cannot participate in SG dynamics, resulting in a weaker response of the SGL changes to SVMC than to ST in the 70–160 cm deep soil layer throughout Period C. Based on the analysis above, it can be inferred that the SG in Period C is primarily recharged by soil water in the shallow layers, and the SGL rise is significantly influenced by thawing depth, dominated by ST in a deeper AL.

As shown in Figure 4d, the relations between SGL and SVMC in the 120–160 cm deep soils agree with the sigmoid formula during Period A (R^2=0.96, P<0.01), while in the 0–90 cm deep soils, the relationship between them could be better described by the Polynomial Cubic formula: $H = H_0 + aM + bM^2 + cM^3$ ($0.85 \leq R^2 \leq 0.96$, P<0.05). As ST continued to decrease during Period A, the liquid water in the AL soil gradually froze into solid water, resulting in the observed SVMC (liquid water content), and the SGL continuously decreased accordingly. Although there was a good relationship between SGL and SVMC at the 120–160 cm depth, the impact of soil moisture below 120 cm on SGL may be limited because SGL drops rapidly from high to low levels with minimal decrease in SVMC below a depth of 120 cm (Figure 4d). When the SGL changed in Period A, the variation range of the SVMC first increased and then decreased from the shallow to deep soil layers. The SVMC range gradually increased from 7–22 % (10 cm) in the shallowest layer to 10–33 % (70 cm) and then gradually decreased to 32–33 % (160 cm). This indicates that the response rate of the SGL to soil moisture first decreased and then increased with depth. By comparing the response rate of SGL to ST changes at different depths during Period A (Figure 4c), it was found that deeper soils in the 0–70 cm soil layer had a larger influence of ST on SGL. Although the SVMC and ST both have good relationships with the SGL below a depth of 70 cm, the variation scope of the SVMC is minimal, and the freezing process of deep soil determines the uplift process of the AL lower boundary, which affects the SGL. Therefore, the deep layer also more directly impacts the SGL owing to the ST.

https://doi.org/10.5194/egusphere-2023-1394
Preprint. Discussion started: 7 July 2023

Figure 5 shows the changes in SGL and ST as well as SGL and SVMC in the AL at different depths during Period D. The range of ST fluctuations gradually decreases with increasing AL depth but generally exceeds 2 ℃. Through correlation analysis, we found that the correlation between the ST at different AL depths and the SGL during Period D was very poor (R^2<0.1) (Figure 5a). The SVMC shows an "increase-decrease-increase" process as depth increases. The correlation between SVMC and SGL in the shallow soil was better than that in the deep soil, with the highest correlation observed at a depth of 10 cm (R^2=0.52) (Figure 5b). This indicates that during Period D (also the stable thawing period of AL), the SGL was more sensitive to SVMC changes in the shallow AL (0–30 cm). The remaining depths of the AL and SGL were not sensitive to either ST or SVMC changes during Period D, when SGL fluctuated at high values for an extended duration and deep soil water remained predominantly saturated or nearly saturated. According to the rainfall process during this period (Figure 2), the dynamics of the SGL were primarily affected by rainfall, which could rapidly recharge the water storage in shallow soils and subsequently affect the SGL.

5 Linkage between river discharge and SGL

To further analyze the impact of SG on river runoff, Figure 6 shows the relationship between SGL and RL in the SL and FHS river basins during Periods C and D, respectively. In both the SL and FHS watersheds, the SGL and RL processes were similar (Figure 6a, 6c). As shown in Figure 6a, the SGL and RL showed stable fluctuations in the SL watershed during June 15–July 18 (Period C) and July 19–August 24 (early Period D), and the consistency of the “SGL-RL” process was very high. However, compared with early Period D, the consistency of the SGL and RL process changes in Phase C was slightly poor (R^2=0.13, P<0.05), which may have been caused by the different AL thawing process and the recharge of snowmelt water to river runoff. In Period D, the dynamic process of SGL was highly consistent with the regression and flood processes of river runoff, with a high correlation (R^2=0.57, P<0.01). It can be inferred that the SWL contributed to approximately 57.0 % of the RL changes in Period D in the SL watershed (Figure 6b). Compared with Period C, the consistency in Period D was superior, and the regression and flood processes were quicker.

Similar to the SL watershed, the SGL and RL in the FHS watershed had consistent fluctuations from August 31–October 18 (Period D). Both showed a significant downward trend from October 2 (late Period D), and their curves were in good agreement (Figure 6c). It can be inferred from Figure 6d that the SWL contributed approximately 65.8 % of the RL changes in Period D in the FHS watershed. However, the rate of decrease in SGL was larger than that of RL. The decrease in SG was larger than 0.3 m, while that of RL was approximately 0.12 m. This may be because the surface soil begins to gradually freeze with temperature drops in late Period D when the river water can be recharged by rainfall or snowmelt water. The freezing of shallow soil weakens the hydraulic connection between AL and the land surface, resulting in poorer water recharge conditions, fewer water supply sources for AL, and a relatively large decrease in SGL.

https://doi.org/10.5194/egusphere-2023-1394
Preprint. Discussion started: 7 July 2023

6 Framework of watershed hydrology responding to the freeze–thaw of AL

According to the above analysis, the yearly hydrothermal changes have four distinct periods with seasonal AL freezing and thawing. The characteristics of the AL depth, SVMC, SGL, and surface RL changes in the four periods varied significantly (Figure 7). In Period A, ST rapidly decreased, leading to the upper layer and the bottom of the AL to begin freezing approximately simultaneously, which resulted in the limit of the external water supply to the AL. Then, the SGL rapidly decreased and reached the minimum value, as the surface RL also decreased rapidly. However, because of the recharge of rainfall runoff or snowmelt runoff, the rate of decline of RL was relatively slower than that of SGL. In Period B, the ST was stably low, the AL was entirely frozen, and the SGL dropped to the lowest level with small changes. The RL changes were not consistent with the SGL at all times during the period. When snowmelt water recharge occurs, RL significantly increases, and the runoff process fluctuates and changes accordingly. In Period C, the warming of the air temperature led to rapid downward thawing of the AL from the surface, resulting in the SGL rising rapidly and reaching its maximum value. Affected by the recharge of the lateral outflow of the SGL and rainfall runoff, the RL also rose rapidly. In Period D, high temperatures led to the deepest AL thawing. During this period, SGL and RL were significantly affected by rainfall. The SGL can increase rapidly with rainfall events during the rainy season and maintain a higher value for a year with small fluctuations. In late Period D, when rainfall decreases, or no rain occurs, the SGL rapidly falls, and the river runoff is primarily recharged by a small amount of SG flowing out from AL, resulting in RL falling back to a low value. When snowfall occurs in late autumn, snowmelt recharges river runoff and causes the RL to rise. In addition, river runoff reverses the recharge of the SG, leading to a moderate increase in the SGL. Under the scenario of continuous warming in the future, AL will be thicker, and the precipitation processes and vegetation underlying surfaces will change, leading to a more complex water regulatory mechanism of AL change.

7 Discussion

SG has a crucial impact on runoff formation processes and water resource changes in permafrost regions. This study analyzed the hydrothermal changes in AL at four different locations on the Qinghai–Tibet Plateau as well as the relationship between ST (SVMC) and SGL. We preliminarily clarified the impact of the seasonal freeze–thaw process of AL on the SG and surface RL in the permafrost watershed, which helps improve the understanding of permafrost hydrological research. However, some shortcomings remain and require further improvement in the current research, especially regarding the observation accuracy of the SGL. Some errors always occur in SGL field experiments on some observations, and some major existing experimental methods, such as the pumping water method, water level gauge method, and radar detection method, make it difficult to accurately measure SGL changes (Yao, 2010). Furthermore, SGL is directly affected by the freeze–thaw process of AL, which complicates SGL change, especially in the rapid melting and freezing stages, thus increasing the difficulty and errors of SGL observation. Therefore, it is necessary to develop innovative instruments and observation methods to improve the accuracy of SGL observations. In addition, considering the effect of ST changes at

https://doi.org/10.5194/egusphere-2023-1394
Preprint. Discussion started: 7 July 2023

different depths, with or without rainfall, and whether soil moisture content is saturated in the observation, it can more accurately depict the SGL process at different freeze–thaw periods and thus more accurately evaluate the impact of SGL on watershed hydrology.

SGL is a crucial recharge source for baseflow, especially in cold and alpine mountainous areas, where it accounts for a large proportion of baseflow. In several permafrost watersheds on the Qinghai–Tibet Plateau, such as the Heihe and Shule River basins in the Qilian Mountains, the intensity of summer rainfall is relatively low. During this rainfall process, the proportion of direct rainfall-runoff was relatively small, and most of the rainfall first infiltrated the soil of the AL. Owing to the water barrier function of permafrost at the bottom of the AL, most of the infiltrated rainwater is stored in the AL. Some are transported as lateral flows, then flow out in low-lying areas of the watershed or recharge the river runoff with spring water, and some are temporarily stored in the soil to recharge and affect the next rainfall flood (Bosson et al., 2013). The AL is a major phreatic zone in watersheds of cold regions, and its lateral flow plays a distinct role in supplying river runoff (Bense et al., 2009; Fischer et al., 2017). Therefore, quantitative estimation of the water volume of the SGL and its regulation and contribution to river runoff are urgent issues that must be addressed in permafrost hydrological research. Several methods, such as isotope tracing and model simulation, have been applied in SG research and have made progress (Clark et al., 2001; Mavromatis et al., 2014; Huang et al., 2020). However, current fixed-point observations and analyses have limitations, and the quantitative analysis of the recharge of SGL to river runoff in a basin requires model simulation for analysis on a larger scale.

In addition, two distinct high-water soil layers exist in the AL during summer: a shallow layer (0–90 cm depth) and a deep layer (from 110 cm depth to the bottom of the AL), with a dry layer (90–110 cm depth) generally present in the middle AL (Figure 4). This phenomenon could be related to rainfall characteristics, vegetation root depth, water-holding capacity of the soil at different depths, soil type, and soil composition. A shallow soil layer with high moisture content is closely related to abundant summer rainfall. It can be preliminarily estimated that the vertical infiltration of rainfall on the Qinghai–Tibet Plateau can reach up to approximately 90 cm underground during a rainfall event, and soil layers of 0–90 cm depth are also the primary root distribution depths of alpine vegetation. The soil in the middle AL often has a large amount of sand and gravel and poor water-holding capacity. A large supply of gravity water and fissure water, coupled with the water-resisting effect of the permafrost table, leads to a high even saturated SVMC in the deep layer of the AL and causes the deep AL to be a major SG existing region that supplies water to rivers through lateral flow. This hydrological phenomenon also exists in permafrost regions at high latitudes, particularly in the pan-Arctic (Koch, 2016; Manasypov et al., 2020), and presents significant challenges for hydrothermal analysis and simulation in permafrost regions.

https://doi.org/10.5194/egusphere-2023-1394
Preprint. Discussion started: 7 July 2023

8 Conclusions

This study analyzed the seasonal dynamics of SG and the correlations between SGL, ST, SVMC, and RL at different stations on the Qinghai–Tibet Plateau. The variation process of the SGL during a hydrological year can be distinctly divided into four periods: a rapid falling period (October–middle November) (A), a stable low-water period (late November–May) (B), a rapid rising period (approximately June) (C), and a stable high-water period (July–September) (D). This synchronously corresponds to the ST and SVMC variations in AL, which experience a rapid freezing period, frozen stability period, rapid thawing period, and thawing stability period during periods A–D of the SGL, respectively.

ST and SVMC in AL were the primary impact factors of SGL changes in permafrost watersheds, whereas the impact varied in the four different periods. Compared with the other periods, the SGL in Period D was permanently higher. The correlations between SGL and ST, as well as between SGL and SVMC, were relatively poor, and the SGL change responded well to rainfall. During Periods A and C, SGL had a good nonlinear correlation with ST and SVMC in the AL, while the correlations varied at different depths. During Period C, when AL rapidly melted, SVMC in the shallow soils (0–50 cm depth) had a better correlation with SGL, whereas ST in deeper soils of AL (below 50 cm) showed closer relations with SGL than with SVMC. It can be inferred that SG in Period C was primarily recharged by soil water in shallow layers, and the SGL rise was significantly influenced by the thawing depth dominated by ST in deeper AL. In Period A, there is a significant nonlinear correlation between SGL and ST at different depths of the AL ($0.81 \leq R^2 \leq 0.98$, $P<0.05$). As depth increases in the AL, the impact of the SVMC on the SGL weakens, whereas ST gradually becomes the dominant factor affecting the SGL.

According to the comparative analysis, the retreat and flood processes of river runoff were consistent with the SGL changes in Periods C and D, which are the primary annual runoff periods in permafrost basins. The RL dynamics were closely related to the SGL changes during the two periods. The SG and river runoff are interconnected, and their water linkages are significantly affected by the freeze–thaw state of AL. The SWL contributed approximately 10.0 % of the RL changes in Period C, while in Period D, approximately 57.0–65.8 % of the surface runoff in permafrost watersheds was recharged by SG, primarily by rainfall infiltration. The SG is a crucial and potential water source for alpine permafrost watersheds.

In summary, the characteristics of SG at different periods of the year vary, and they have a crucial regulatory effect on the hydrology of permafrost watersheds. With continuous climate warming, the AL will thicken, and the potential precipitation and alpine vegetation also will change. The change mechanism of SGL will correspondingly become more complex and require further research.

Author contribution

Jia Qin and Yongjian Ding developed the idea and outlines of the article. Jia Qin prepared the manuscript with contributions from all co-authors.

https://doi.org/10.5194/egusphere-2023-1394
Preprint. Discussion started: 7 July 2023

Competing interests

The authors declare that they have no conflict of interest.

Acknowledgments

This work was supported by the National Key R&D Program of China (Grant No. 2021YFC3201102-02), the National Natural Science Foundation of China (Grant No. 42171028 and 41877156), the State Key Laboratory of Frozen Soil Engineering Foundation (Grant No. SKLFSE202110), and the Open Project of the State Key Laboratory of Cryospheric Science, China (Grant No. SKLCS-OP-2020-7).

References

Bense, V.F., Ferguson, G., Kooi, H.: Evolution of shallow groundwater flow systems in areas of degrading permafrost. Geophys. Res. Lett., 36, L22401. https://doi.org/10.1029/2009GL039225. 2009.

Bosson, E., Selroos, J.O., Stigsson, M., Gustafsson,, L. G., Destouni, G.: Exchange and pathways of deep and shallow groundwater in different climate and permafrost conditions using the Forsmark site, Sweden, as an example catchment. Hydrogeol. J., 21, 225–237. https://doi.org/10.1007/s10040-012-0906-7. 2013.

Chang, J., Wang, G. X., Li, C. J., Mao, T.: Seasonal dynamics of suprapermafrost groundwater and its response to the freeing-thawing processes of soil in the permafrost region of Qinghai-Tibet Plateau, Sci. China Earth Sci., 58, 727–738. https://doi.org/10.1007/s11430-014-5009-y, 2015.

Chen, R. S., Wang, G., Yang, Y., Liu, J., Han, C., Song, Y., Liu, Z., Kang, E.: Effects of cryospheric change on alpine hydrology: combining a model with observations in the upper reaches of the Hei River, China, J. Geophys. Res. Atmos., 123, 3414–3442. https://doi.org/10.1002/2017JD027876, 2018.

Clark, I. D., Lauriol, B., Harwood, L., Marschner, M.: Groundwater contributions to discharge in a permafrost setting, Big Fish River, N.W.T., Canada, Arct. Antarct. Alp. Res., 33, 62–69. https://doi.org/10.1080/15230430.2001.12003405, 2001.

Dahe, Q., Tandong, Y., Yongjian, D., Jiawen, R.: Glossary of cryospheric science （revised edition）[M], China Meteorological Press, Beijing， 2016.

Dugan, H. A., Lamoureux, S. F., Lafrenière, M. J., Lewis, T.: Hydrological and sediment yield response to summer rainfall in a small high Arctic watershed, Hydrol. Process, 23, 1514–1526. https://doi.org/10.1002/hyp.7285, 2009.

Fischer, B.M.C., Stahli, M., Seibert, J.: Pre-event water contributions to runoff events of different magnitude in pre-alpine headwaters. Hydrol. Res., 48, 28–47. https://doi.org/10.2166/nh.2016.176. 2017.

Gao, Z., Niu, F. J., Wang, Y. B., Lin, Z., Wang, W.: Suprapermafrost groundwater flow and exchange around a thermokarst lake on the Qinghai-Tibet Plateau, China, J. Hydrol., 593, 125882. https://doi.org/10.1016/j.jhydrol.2020.125882, 2021.

https://doi.org/10.5194/egusphere-2023-1394
Preprint. Discussion started: 7 July 2023

Ge, S., McKenzie, J., Voss, C., Wu, Q.: Exchange of groundwater and surface-water mediated by permafrost response to seasonal and long term air temperature variation, Geophys. Res. Lett., 38 http:, n/a–n/a. https://doi.org/10.1029/2011GL047911, 2011.

Hongliang, X., Juan, C., Linmao, G., Wenjun, S., et al.: Response of thermal-moisture condition within active layer in the hinterland of the Qinghai-Xizang Plateau to climate change［J］, Plateau Meteorol.，40（2）：229-243, 00071, 1000–0534. 2020. https://doi.org/10.7522/j.issn, 2021.

Huang, K., Dai, J., Wang, G., Chang, J., Lu, Y., Song, C., Hu, Z., Ahmed, N., Ye, R.: The impact of land surface temperatures on suprapermafrost groundwater on the central Qinghai-Tibet Plateau, Hydrol. Processes, 34, 1475–1488. https://doi.org/10.1002/hyp.13677, 2020.

Koch, J. C.: Lateral and subsurface flows impact arctic coastal plain lake water budgets, Hydrol. Process., 30, 3918–3931. https://doi.org/10.1002/hyp.10917, 2016.

Koch, J. C., Sjöberg, Y., O'Donnell, J. A., Carey, M. P., Sullivan, P. F., Terskaia, A.: Sensitivity of headwater streamflow to thawing permafrost and vegetation change in a warming Arctic, Environ. Res. Lett., 17, 044074. https://doi.org/10.1088/1748-9326/ac5f2d, 2022.

Krickov, I. V., Lim, A. G., Manasypov, R. M., Loiko, S. V., Shirokova, L. S., Kirpotin, S. N., Karlsson, J., Pokrovsky, O. S.: Riverine particulate C and N generated at the permafrost thaw front: case study of western Siberian rivers across a 1700 km latitudinal transect, Biogeosciences, 15, 6867–6884. https://doi.org/10.5194/BG-15-6867-2018, 2018.

Lebedeva, L.: Tracing surface and ground water with stable isotopes in a small permafrost research catchment. E3S web of conferences. https://doi.org/10.1051/e3sconf/201912405088, 2019.

Liu, W., Fortier, R., Molson, J. W., Lemieux, J.: A conceptual model for talik dynamics and icing formation in a river floodplain in the continuous permafrost zone at Salluit, Nunavik (Quebec), Canada, Permafrost Periglacial Processes, 32, 468–483. https://doi.org/10.1002/ppp.2111, 2021.

Ma, R., Sun, Z., Hu, Y.Chang, Q., Ge, M.: Hydrological connectivity from glaciers to rivers in the Qinghai–Tibet Plateau: roles of suprapermafrost and subpermafrost groundwater, Hydrol. Earth Syst. Sci. Discuss., 1–39. https://doi.org/10.5194/hess-2017-7, 2017.

Manasypov, R. M., Lim, A. G., IV, Krickov, I. V., Shirokova, L. S., Vorobyev, S. N., Kirpotin, S. N., Pokrovsky, O. S.: Spatial and seasonal variations of C, nutrient, and metal concentration in Thermokarst Lakes of western Siberia across a permafrost gradient, Water, 12, 1830. https://doi.org/10.3390/w12061830, 2020.

Mavromatis, V., Prokushkin, A. S., Pokrovsky, O. S., Viers, J., and Korets, M. A.: Magnesium isotopes in permafrost-dominated Central Siberian larch forest watersheds, Geochim. Cosmochim. Acta, 147, 76–89. https://doi.org/10.1016/j.gca.2014.10.009, 2014.

O'Connor, M. T., Cardenas, M. B., Neilson, B. T., Nicholaides, K. D., Kling, G. W.: Active layer groundwater flow: the interrelated effects of stratigraphy, thaw, and topography, Water Resour. Res., 55, 6555–6576. https://doi.org/10.1029/2018WR024636, 2019.

https://doi.org/10.5194/egusphere-2023-1394
Preprint. Discussion started: 7 July 2023

O'Neill, H. B., Roy-Leveillee, P., Lebedeva, L., Ling, F.: Recent advances (2010–2019) in the study of taliks, Permafrost Periglacial Processes, 31, 346–357. https://doi.org/10.1002/ppp.2050, 2020.

Qin, J., Ding, Y. J., Han, T. D., Chang, Y., Shi, F., You, Y.: The hydrothermal changes of permafrost active layer and their impact on summer rainfall-runoff processes in an alpine meadow watershed, Northwest China, Research in Cold and Arid Regions, 14, 361–369. https://doi.org/10.1016/j.rcar.2023.02.005, 2022.

Raudina, T. V., Loiko, S. V., Lim, A., Manasypov, R. M., Shirokova, L. S., Istigechev, G. I., Kuzmina, D. M., Kulizhsky, S. P., Vorobyev, S. N., Pokrovsky, O. S.: Permafrost thaw and climate warming may decrease the CO2, carbon, and metal concentration in peat soil waters of the Western Siberia Lowland, Sci. Total Environ., 634, 1004–1023. https://doi.org/10.1016/j.scitotenv.2018.04.059, 2018.

Renzheng, Y. and Juan, C.: Study of groundwater in permafrost regions of China: status and process［J］, J. Glaciol. Geocryol., 41, 183–196. https://doi.org/10.7522/j.issn.1000-0240.2019.0009, 2019.

Schuur, E. A. and Abbott, B.: Climate change: High risk of permafrost thaw, Nature, 480, 32–33. https://doi.org/10.1038/480032a, 2011.

Sjöberg, Y., Frampton, A., and Lyon, S. W.: Using streamflow characteristics to explore permafrost thawing in northern Swedish catchments, Hydrogeol. J., 21, 121–131. https://doi.org/10.1007/s10040-012-0932-5, 2013.

Throckmorton, H. M., Newman, B. D., Heikoop, J. M., Perkins, G. B., Feng, X., Graham, D. E., O'Malley, D., Vesselinov, V. V., Young, J., Wullschleger, S. D., Wilson, C. J.: Active layer hydrology in an arctic tundra ecosystem: quantifying water sources and cycling using water stable isotopes, Hydrol. Process., 30, 4972–4986. https://doi.org/10.1002/hyp.10883, 2016.

Tregubov, O. D., Gartsman, B. I., Shamov, V. V., Lebedeva, L. S., and Tarbeeva, A. M.: The effect of atmospheric pressure variations on the suprapermafrost groundwater level and runoff of Small Rivers in the Anadyr lowlands, Northeast Russia, Water, 14, 3066. https://doi.org/10.3390/w14193066, 2022.

Tregubov, O. D., Gartsman, B. I., Tarbeeva, A. M., Lebedeva, L. S., Shepelev, V. V.: Spatial and temporal dynamics of sources and water regime of the Ugol'naya-Dionisiya river (Anadyr Lowland, Chukotka), Water Resour., 48, 521–531. https://doi.org/10.1134/S0097807821040187, 2021.

Walvoord, M. A., Voss, C. I., and Wellman, T. P.: Influence of permafrost distribution on groundwater flow in the context of climate-driven permafrost thaw: example from Yukon Flats Basin, Alaska, United States, Water Resour. Res., 48, 7524. https://doi.org/10.1029/2011WR011595, 2012.

Wang, G. X., Liu, G. S., Li, C. J., Yang, Y.: The variability of soil thermal and hydrological dynamics with vegetation cover in a permafrost region. Agric. For. Meteorol., 162-163, 44–57. http://doi.org/10.1016/j.agrformet.2012.04.006. 2012.

Wei, C., Sheng, Y., Jichun, W., Shengting, W., Shuai, M.: Seasonal variation of soil hydrological processes of active layer in source region of the Yellow River, Adv. Water Sci., 29, 1–10, 1309. https://doi.org/10.14042/j. cnki. 32, 2018. 01. 001.

https://doi.org/10.5194/egusphere-2023-1394
Preprint. Discussion started: 7 July 2023

Wei, C., Yu, S., Jichun, W., Yaling, C., Erxing, P., Leonid, G.: Soil hydrological process and migration mode influenced by the freeze-thaw process in the activity layer of permafrost regions in Qinghai-Tibet Plateau, Cold Reg. Sci. Technol., 184, 103236. https://doi.org/10.1016/j.coldregions.2021.103236, 2021.

Wellman, T. P., Voss, C. I., and Walvoord, M. A.: Impacts of climate, lake size, and supra- and sub-permafrost groundwater flow on lake-talik evolution, Yukon Flats, Alaska (USA), Hydrogeol. J., 21, 281–298. https://doi.org/10.1007/s10040-012-0941-4, 2013.

Wenbing, C.,Wan Li,,Zhou Xun, et al: A study of the geological environmental of suprapermafrost water in the headwater area of the Yellow River, Hydrogeol. Eng. Geol., 6, 6–10. https://doi.org/10.3969/j.issn.1000-3665.2003.06.002, 2003.

Woo, M. K. and Xia, Z.: Suprapermafrost groundwater seepage in gravelly terrain, resolute, NWT, Canada, Permafrost Periglacial Process., 6, 57–72. https://doi.org/10.1002/ppp.3430060107, 1995.

Yongxi, Y.: Summarization on monitoring methods & instrument for UndergroundWater, Autom. Water Resour. Hydrol., 1, 6–13, 2010.

Young, K. L. and Mingko, W.: Hydrological response of a patchy high arctic wetland, Nord. Hydrol., 31, 317–338. https://doi.org/10.2166/nh.2000.0019., 2000.

Zhang, M., Wen, Z., Li, D., Chou, Y., Zhou, Z., Zhou, F., Lei, B.: Impact process and mechanism of summertime rainfall on thermal–moisture regime of active layer in permafrost regions of central Qinghai–Tibet Plateau, Sci. Total Environ., 796, 148970. https://doi.org/10.1016/j.scitotenv.2021.148970, 2021.

https://doi.org/10.5194/egusphere-2023-1394
Preprint. Discussion started: 7 July 2023

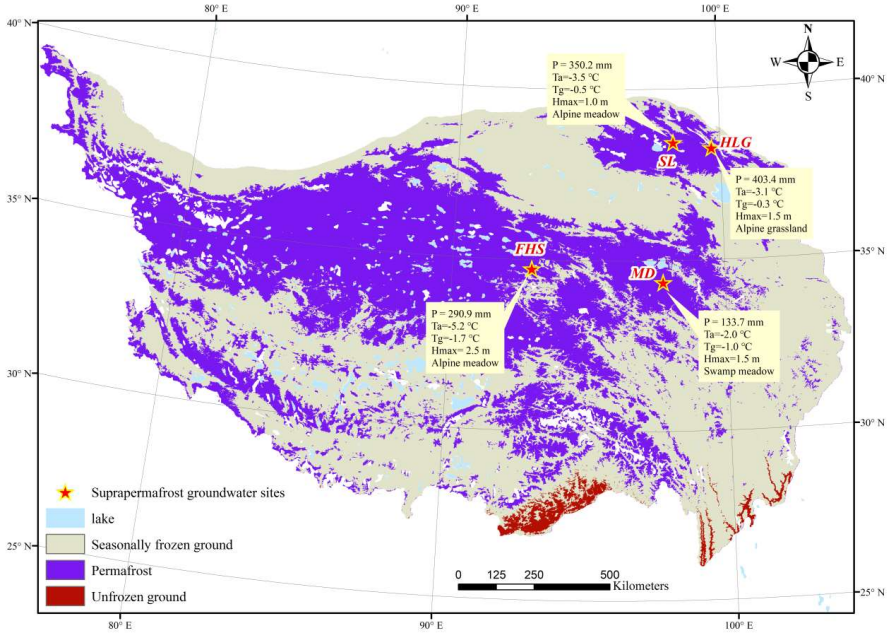

455 **Figure 1: Permafrost distribution and locations of the four SG observation stations in the Qinghai–Tibet Plateau. P is the annual precipitation, Ta is the annual mean air temperature, Tg is the annual mean ground temperature, and Hmax is the maximum yearly depth of AL.**

https://doi.org/10.5194/egusphere-2023-1394
Preprint. Discussion started: 7 July 2023

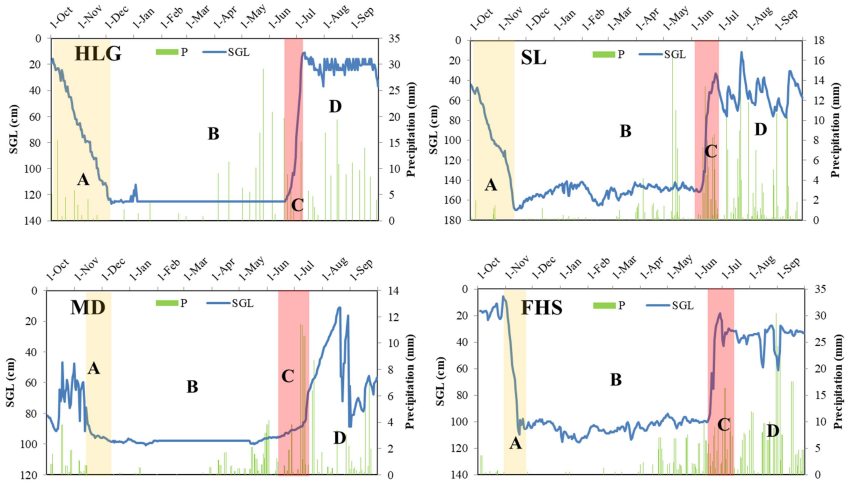

460 **Figure 2: Four major phases of the seasonal suprapermafrost groundwater level (SGL) and the corresponding daily precipitation (P) in different sites of the Qinghai–Tibet Plateau. A–D refer to the rapid falling period, stable low-water period, rapid rising period, and stable high-water period, respectively.**

https://doi.org/10.5194/egusphere-2023-1394
Preprint. Discussion started: 7 July 2023

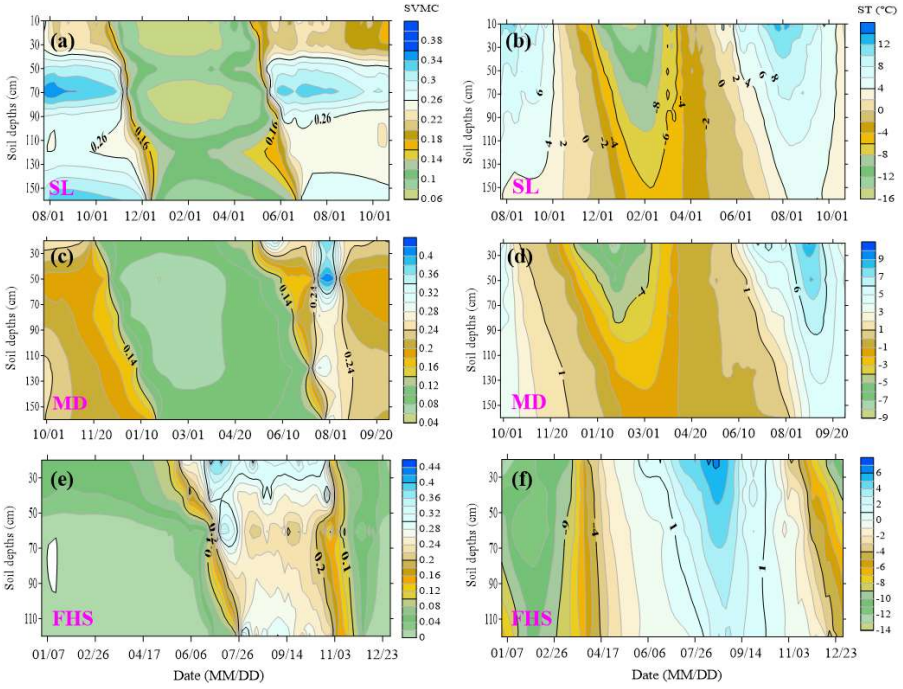

Figure 3: Vertical variations in soil temperature (ST) and soil volumetric moisture content (SVMC) in the different sites of the Qinghai–Tibet Plateau.

https://doi.org/10.5194/egusphere-2023-1394
Preprint. Discussion started: 7 July 2023

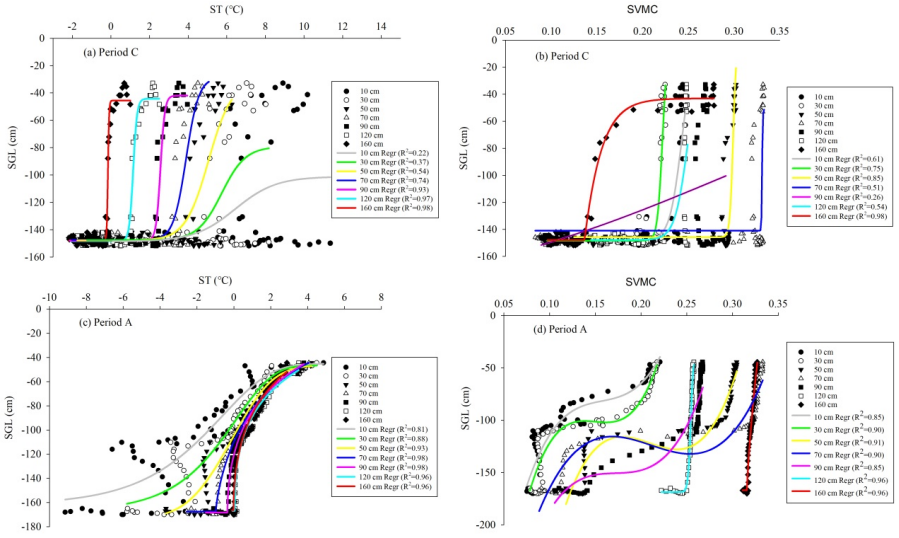

Figure 4: Correlations of SGL and SVMC (ST) in different depths of AL during Periods A and C.

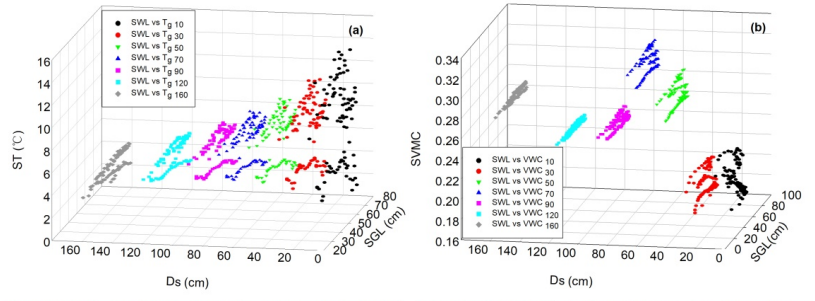

linear regression: SGL vs. ST	10 cm	30 cm	50 cm	70 cm	90 cm	120 cm	160 cm
R^2	0.04	0.05	0.06	0.07	0.08	0.07	0.04
P				<0.001			

linear regression: SGL vs. SVMC	10 cm	30 cm	50 cm	70 cm	90 cm	120 cm	160 cm
R^2	0.52	0.15	0.07	0.05	0.10	0.09	0.04
P				< 0.001			

Figure 5: Variations and correlations of SGL and ST (a) as well as SGL and SVMC (b) in different depths (Ds) of the permafrost active layer in Period D.

https://doi.org/10.5194/egusphere-2023-1394
Preprint. Discussion started: 7 July 2023

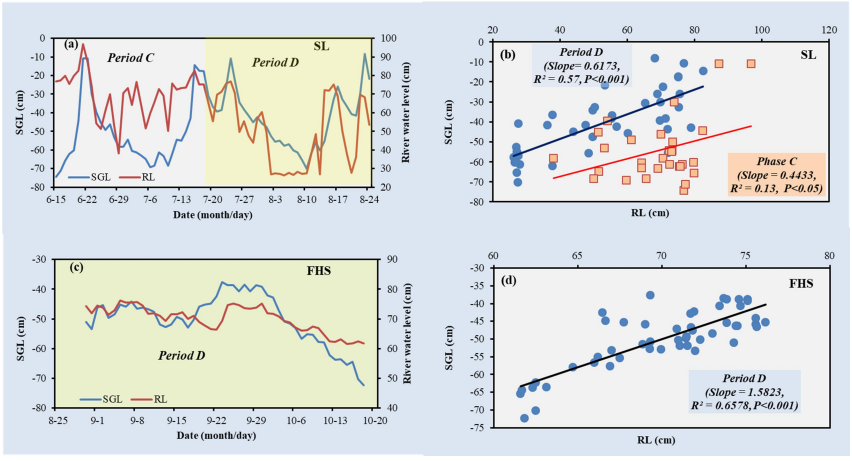

Figure 6: Variations of SGL (a, c) and the correlations between SGL and river level (RL) (b, d) in Periods C and D, respectively, in the SL and FHS watersheds.

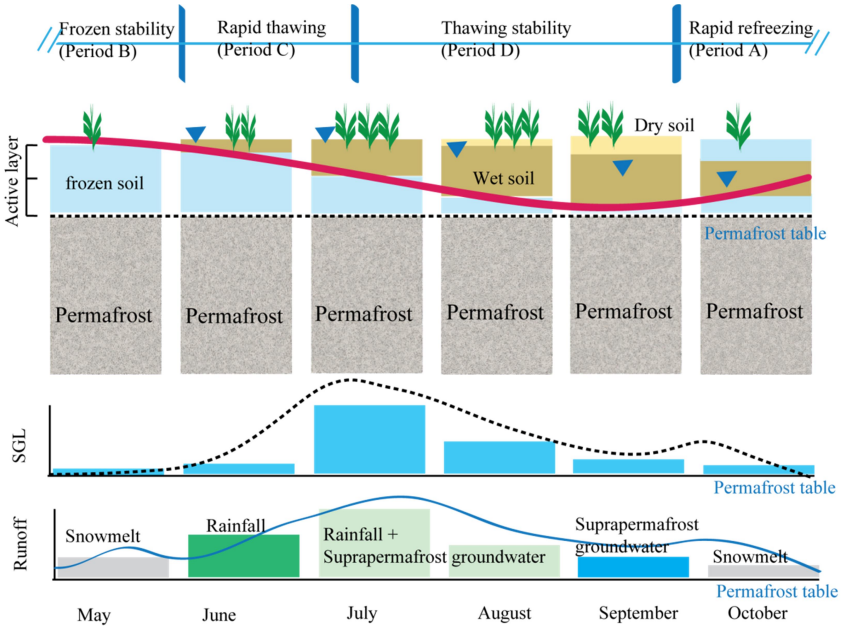

Figure 7: Framework of watershed hydrology responding to the freeze–thaw of the permafrost active layer.